IMPROVEMENT OF SLIPPAGE AND WRINKLING OF TRANSPORTING WEBS USING MICRO-GROOVED ROLLERS

By

Hiromu Hashimoto[1] and Shinji Hikita[2]
[1]Tokai University
[2]Fujifilm Corporation
JAPAN

ABSTRACT

We describe an entirely new method of improving the slippage between web and roller. First, the concept of a micro-grooved roller is introduced, and then a theoretical model for estimating the slip onset velocity under the transport of web by the micro-grooved roller is formulated. The predicted results are compared with the experimental data to verify the applicability of the prediction model of slippage. Moreover, the web-wrinkling condition, which is in a trade-off relationship with the slippage condition, is also considered in the model. From the theoretical and experimental results, it is confirmed that the optimized micro-grooved roller is very effective in improving the slippage and wrinkling of thin web under the high-speed transport with low tension at the actual production line.

INTRODUCTION

The demand for liquid crystal displays (LCDs) in recent years is markedly increasing, whereas the price of LCD panels decreases. Therefore, a high productivity, more specifically a manufacturing technology that enables mass production at a low cost but a high quality, is required to produce high-functional webs, such as optical films used in LCDs. As concrete measures to increase the productivity, for example, the manufacturing speed of the conventional production lines should be increased, and thinner webs should be manufactured to reduce the cost of raw materials without losing the established high quality functions.

In the manufacturing process, webs are transferred by the traction between the web and roller. As the production speed increases, the amount of entrained air into the gap between the web and roller also increases, which is causing the traction loss and slippage. Slippage sometimes causes surface scratches and meandering of webs. Therefore, the manufactures of webs should avoid such web defects to keep the quality in the production lines. In particular, even a tiny scratch of micron scale is not permitted on an optical film for LCDs. To protect the traction loss due to air entrainment, it has been experimentally

used to increase the web tension. However, when we want to avoid the slippage by this way, web wrinkling easily generate in the process, so it is required to discover the novel method for preventing both slippage and wrinkling simultaneously, which is typical trade-off problem in the web handling industries.

Until now, very few papers, treating such problem from the academic side, are available in the literatures [1-3]. Among them, Hashimoto[1] originally demonstrated the idea of using the micro-grooved roller to improve the traction loss due to air entrainment and showed the effectiveness of the roller by the parametric study. However, the applicability of the micro-grooved roller to the actual web handling system was not verified experimentally. Regarding to the web wrinkling problems, Good et al.[2] formulated the prediction model for generating the wrinkling of isotropic web. Hashimoto[3] extended this model to the anisotropic webs and compared the predicted results with the measured data to verify the applicability of the model. But the trade-off relation between the slippage and wrinkling are not sufficiently clarified yet.

In this paper, the theoretical modeling for predicting the slippage and wrinkling is described for micro-grooved rollers and the optimization method for designing the effective micro-grooved rollers to prevent these web defects is formulated with experimental verifications. Moreover, an example of an application of this model to the actual web production line is introduced.

NOMENCLATURE

a	inter-axial distance of the roller (m)
b_g	groove width (m)
E_x	Young's modulus in the machine direction (GPa)
E_z	Young's modulus in the cross machine direction (GPa)
F	traction between the web and roller (N)
f	bearing resistance of rotation (N)
$f(\boldsymbol{X})$	objective function
$g_i(\boldsymbol{X})$	constraint functions (i=1～7)
h	air film thickness (m)
h_{eq}	equivalent air film thickness (m)
h_g	groove depth (m)
I	Inertia moment of the roller (kg m^2)
n_g	number of micro-grooves
q_x	amount of air film flow (m^3/s)
p_{cr}	critical pressure to prevent from scratch (Pa)
p	pressure between the web and roller (Pa)
R	roller radius (m)
r	bearing radius (m)
s	slip ratio
s_g	cross-sectional area of micro-groove (m^2)
T	inlet web tension (N/m)
T'	outlet web tension (N/m)
T_{cr}	critical web tension to generate wrinkling (N/m)
T_{slip}	slip onset tension (N/m)
t_w	web thickness (m)
U	combined velocity between the web and roller velocities (m/s) (=U_w +U_r)
U_w	web velocity (m/s)
U_r	roller surface velocity (m/s)
U_{slip}	slip onset velocity (m/s)

W	web width (m)
$\boldsymbol{X}$	design variable vector
η	air viscosity (Pa s)
Θ	wrap angle (rad)
θ	misalignment angle of the roller (rad)
θ_{cr}	critical misalignment angle of the roller (rad)
μ_{eff}	effective friction coefficient including air film effect
μ_{slip}	friction coefficient at the onset of slippage
μ_s	static friction coefficient between the web and roller
ν_x , ν_z	Poisson's ratio of the web in the machine and cross machine directions
ρ	density of air (kg/m^3)
σ	combined *rms* roughness between the web and roller (m)
σ_{zcr}	critical buckling stress in the cross machine direction (Pa)
σ_x	normal stress in the machine direction (= T/t_w) (Pa)
$\dot{\omega}$	angular acceleration of the roller (rad/s^2)

AIR FILM THICKNESS ESTIMATION FOR MICRO-GROOVED ROLLER

Air film thickness estimation for non-grooved roller

For the purpose of improving the traction characteristics between the web and roller, it is needed first to predict the entrained air film thickness. Before formulating the micro-grooved roller theory to predict the traction between the web and roller, the traditional foil bearing model, that gives the simplified formula for evaluating the entrained air film thickness between the web and non-grooved roller, is described briefly in the following.

In the foil bearing model as shown in Figure 1, the width of web W is generally larger than the roller diameter $2R$, and then the air film flow can be treated as one-dimensional in the x-direction. Under such situation, the nonlinear Reynolds equation and the web elastic equation are given, respectively as follows.

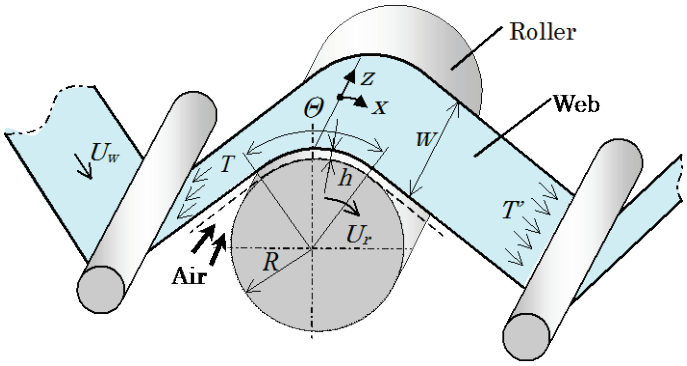

Figure 1 – Foil bearing model

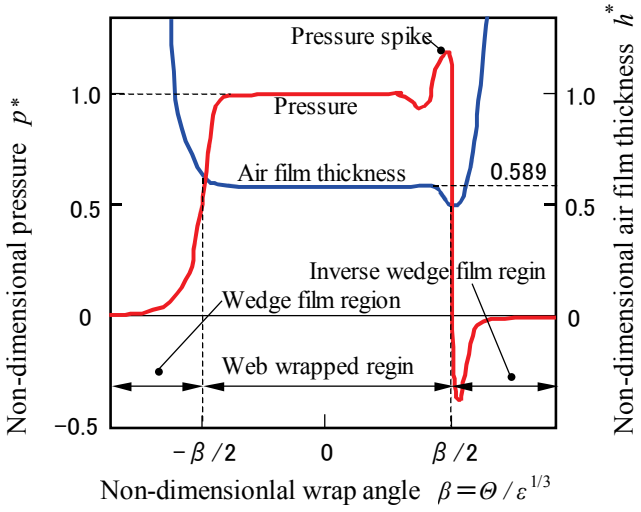

Figure 2 – Air film thickness and pressure distributions for non-grooved roller

$$\frac{d}{dx}\left(h^3 p\frac{dp}{dx}\right)=6\eta U\frac{d(ph)}{dx} \quad ; \quad U=U_r+U_w \tag{1}$$

$$\frac{Et_w^{\,3}}{12(1-\nu_x^{\,2})}\frac{d^4h}{dx^4}+\frac{T}{R}\left(1-R\frac{d^2h}{dx^2}\right)=p-p_a \tag{2}$$

In the case of very thin webs treated in this paper, the first term of the left hand side in equation {2} can be neglected, and equation {2} is reduced to the following equation.

$$\frac{T}{R}\left(1-R\frac{d^2h}{dx^2}\right)=p-p_a \tag{3}$$

Solving equations {1} and {3} simultaneously with the proper boundary conditions on p and h, the pressure and air film thickness distributions are obtained as shown in Figure 2, in which the non-dimensional quantities are introduced as follows.

$$p^*=\frac{p}{T/R}\,,\quad h^*=\frac{h}{R\varepsilon^{2/3}}\,,\quad \varepsilon=\frac{6\eta U}{T}\,,\quad \beta=\frac{\Theta}{\varepsilon^{1/3}} \tag{4}$$

As can be seen in the figure, in the web wrapped region the non-dimensional pressure p^* becomes the constant value of $p^*\cong 1$ and the non-dimensional air film thickness h^* also becomes the constant value of $h^*\cong 0.589$, respectively, which are independent of the non-dimensional wrap angle β, and it was confirmed that such a trend does not change for a wide range of web wrap angle Θ larger than 0 deg. From this fact, the dimensional pressure p and air film thickness h between the web and non-grooved roller are approximately expressed as follows.

$$p = \frac{T}{R} \quad \{5\}$$

$$h = 0.589R\left(\frac{6\eta U}{T}\right)^{\frac{2}{3}} \quad \{6\}$$

Moreover, neglecting the pressure gradient flow in the web wrapped region, the air flow rate per unit width between the web and non-grooved roller is given as follows.

$$q_x = \frac{\rho h U}{2} \quad \{7\}$$

Air film thickness estimation for micro-grooved roller

The concept of micro-grooved roller was introduced originally by Hashimoto[1]. The micro-grooved roller presented in this paper is manufactured a number of micro-size grooves in the circumferential direction of roller surface as shown in Figure 3. In the micro-size grooves, it is considered that the air flow is dominated by the viscous flow and the pressure gradient flow in the web wrapped region can be neglected as in the case of non-grooved roller. Based on such considerations, the air flow rate per unit width between the web and micro-grooved roller is expressed as follows.

$$q_x = \frac{\rho U}{2}(h + \frac{n_g s_g}{W}) \quad \{8\}$$

Introducing the equivalent air film thickness h_{eq} as shown Figure 3, the air flow rate is expressed directly with equation {7} as follows.

$$q_x = \frac{\rho U}{2} h_{eq} = 0.589\frac{\rho R U}{2}\left(\frac{6\eta U}{T}\right)^{\frac{2}{3}} \quad \{9\}$$

Equating equations {8} and {9}, the air film thickness, h, between the web and the top surface of micro-grooved roller, shown in Figure 3, is obtained as follows.

$$h = 0.589R\left(\frac{6\eta U}{T}\right)^{\frac{2}{3}} - \frac{n_g s_g}{W} \quad \{10\}$$

It follows from equation {10} that the air film thickness h can be reduced effectively by suitable designing the groove size, n_g and s_g. When the air film thickness h becomes negative, it should be equated to zero.

The idea of grooved roller itself has been well known for the web handling engineers, but in that case, the groove size is millimeter scale, and therefore we call such type of groove as "macro-groove". As far as the authors know, however, the idea of "micro-groove" to improve the traction characteristics between the web and roller has not been known, except the report by Hashimoto et al.[1].

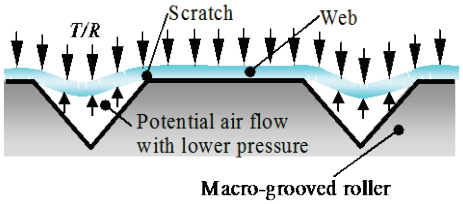

Figure 3 – Concept of micro-grooved roller

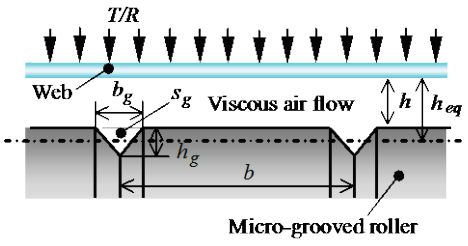

Figure 4 – Concept of macro-grooved roller

Figure 4 shows the conceptual diagram of macro-grooved roller. As the size of macro-grooves is usually millimeter scale as mentioned above, the air flow inside the groove is dominated by the potential flow. In this case, the air flow through the macro-grooves is accelerated and the pressure inside the groove becomes lower than that outside. As a result, the web is easy to deform and sometimes generate scratches as shown in the figure. On the other hand, the pressure inside the micro-groove does not become lower, because the air flow inside the groove is dominated by the viscous flow and adhered to the groove wall, and therefore is not accelerated.

PREDICTION OF SLIPPAGE AND WRINKLING

Figure 5 shows the conceptual diagram of the interface between the web and roller. The effective friction coefficient μ_{eff} , which is including the effect of entrained air as mentioned in the former chapter, is approximately given as follows.

$$\mu_{eff} = \begin{cases} \mu_s & (h < \sigma) \\ \dfrac{\mu_s}{2}\left(3 - \dfrac{h}{\sigma}\right) & (\sigma \le h \le 3\sigma) \\ 0 & (h > 3\sigma) \end{cases} \qquad \{11\}$$

where h is the entrained air film thickness given by equation {10}, and σ is the *rms* composite surface roughness between the web and roller, which is defined in following.

$$\sigma = \sqrt{\sigma_w{}^2 + \sigma_r{}^2} \qquad \{12\}$$

From Figure 5, the slip onset condition between the web and roller is expressed as follows;

$$FR = I\dot{\omega} + fr \qquad \{13\}$$

where $I\dot{\omega}$ means the inertia torque that can be neglected under the steady state condition. The traction, F, transmitted between the web and roller is given by the following relation.

$$F = W(T' - T) \qquad \{14\}$$

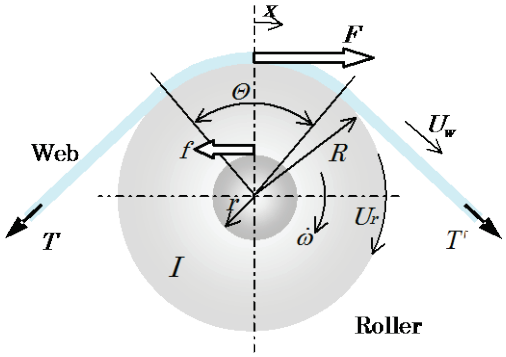

Figure 5 – Traction transmitted from roller to web or from web to roller

From the Euler's belt theory, the relation between T and T' is given as follows.

$$T' = T\, e^{\mu_{eff}\Theta} \qquad \{15\}$$

From equation {13} through equation {15}, the effective friction coefficient to start the slippage is given as follows.

$$\mu_{slip} = \frac{1}{\Theta}\ln\left(1+\frac{I\dot{\omega}+fr}{WRT}\right) \qquad \{16\}$$

Generally, it is considered that the slippage will occur in the mixed lubrication region of $\sigma \le h \le 3\sigma$, and then equating equation {16} to the middle expression in equation {11} after substituting h from equation {10}, the slip onset velocity of roller for the fixed value of tension is obtained by the following equation. At the same time, the slip onset tension for the fixed value of velocity is also obtained by solving the equation with respect to tension, T.

$$U = \frac{1}{12}\left\{5.093-\frac{3.396}{\mu_s\Theta}\ln\left(1+\frac{I\dot{\omega}+fr}{WRT}\right)+1.698\frac{n_g s_g}{\sigma W}\right\}^{\frac{3}{2}}\frac{T}{\eta}\left(\frac{\sigma}{R}\right)^{\frac{3}{2}} \qquad \{17\}$$

When the micro-grooved roller is used for the transport of web, the traction between the web and roller will be greatly improved even in the case of high speed transport with low tension. However, it has been demonstrated by Good[2] and Hashimoto[3] that the wrinkles as shown in Figures 6(a) and 6(b) will be generated due to the misalignment of roller when the sufficient level of friction coefficient is maintained between the web and roller. Especially, in the case of very thin web, like the optical LCD film, the wrinkling is easy to generate and it should be prevented in the production lines.

According to Hashimoto[3], in the mechanism of generating wrinkles, the trough is generated first in the transported web between roller and roller, and after that it leads to wrinkles on the surface of the down stream roller surface, as shown in Figure 6(b). In this paper, the following prediction model[3] developed for the non-grooved roller is also applied to predict the onset of wrinkling for the micro-grooved roller.

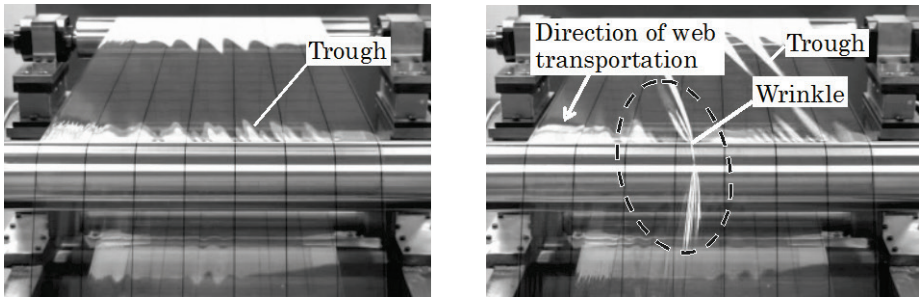

(a) Non-grooved roller (b) Micro-grooved grooved roller

Figure 6 – Observation of wrinkle generation
(U_w=0.15m/s, W=0.3[m], Θ=60[deg], R=0.04[m], T=150[N/m], θ =0.2[deg])

Based on the linearized buckling theory and the energy method, the critical buckling stress in the cross machine direction of the transported web between roller and roller is given by the following equation.

$$\sigma_{zcr} = \frac{W^2}{i^2 a^2}\left\{\sigma_e\left(1+\zeta_1 i^4 \frac{a^4}{W^4}+\zeta_2 i^2 \frac{a^2}{W^2}\right)-\sigma_x\right\} \quad \{18\}$$

where the coefficients ζ_1 and ζ_2 and the stresses σ_x and σ_e are defined, respectively, as follows;

$$\zeta_1 = \frac{E_z}{E_x},\ \zeta_2 = \frac{4(1-\nu_x\nu_z)}{1+\nu_x+(1+\nu_z)/\zeta_1}+\nu_z+\nu_x\zeta_1,\ \sigma_x = \frac{T}{t_w},\ \sigma_e = \frac{\pi^2 E_x {t_w}^2}{12a^2(1-\nu_x\nu_z)} \quad \{19\}$$

and i means the corrugation number to be satisfied with the following inequality.

$$\sigma_e\left\{1-i^2(i+1)^2\zeta_1\frac{a^4}{W^4}\right\} < \sigma_x < \sigma_e\left\{1-(i-1)^2 i^2\zeta_1\frac{a^4}{W^4}\right\} \quad \{20\}$$

When the misalignment angle of the roller, θ, exceeds the critical angle, the trough as shown in Figure 6 will be generated, and the onset condition of trough is expressed as follows.

$$\theta \geq \theta_{cr} = \frac{6a^2}{E_x W^2}\sqrt{{\sigma_{zcr}}^2-\sigma_{zcr}\sigma_x} \quad \{21\}$$

Since the web wrapped over the roller takes the cylindrical form as shown in Figure 6, the critical buckling stress on the roller is given as follows.

$$\sigma_{zcr} = \frac{t_w}{R}\sqrt{\frac{E_x E_z}{3(1-\nu_x\nu_z)}} \quad \{22\}$$

The compressive stress becomes zero at the edges of web width and increases towards the web center with a gradient determined by traction, and then the trough will grow up and leads to generate wrinkling on the center line of web wrapped over the roller, if the following condition is satisfied.

$$\sigma_{zcr} = \mu_{eff} \frac{T_{cr}}{R} \frac{W}{2t_w} \quad \{23\}$$

Substituting equation {22} into equation {23}, the wrinkling onset condition with respect to web tension is obtained as follows.

$$T \geq T_{cr} = \frac{2t_w^{\ 2}}{\mu_{eff} W} \sqrt{\frac{E_x E_z}{3(1-\nu_x \nu_z)}} \quad \{24\}$$

When equations {21} and {24} are satisfied simultaneously, the wrinkles will generate on the center line of web wrapped over the roller.

OPTIMUM DESIGN OF MICRO-GROOVE SIZE

Figure 7 shows one of examples of the predicted results of the slippage and wrinkling regions obtained by the above introduced theory for both cases of non-grooved and micro-grooved rollers. The critical web tension to start the slippage becomes much smaller in the case of micro-grooved roller for the fixed value of the roller velocity, and it means that the web can be transferred successfully with low tension. However, the critical web tension to generate wrinkling also become smaller, and as a result, the safety operation region of micro-grooved roller becomes narrower than that of non-grooved roller. To solve such a serious trade-off problem, it is required to optimize the micro-groove sizes by the following way.

$$\text{Find } \boldsymbol{X} \text{ to minimize } f(\boldsymbol{X}) \text{ subject to } g_i(\boldsymbol{X}) \leq 0 \quad \{25\}$$

where the design vector $\boldsymbol{X}$, objective function $f(\boldsymbol{X})$ and the constraint functions $g_i(\boldsymbol{X})$ are defined, respectively, as follows.

$$\boldsymbol{X} = (b_g, h_g, n_g) \quad \{26\}$$

$$f(X) = \frac{T_{slip}}{T_{cr}} \quad \{27\}$$

$$\left.\begin{aligned} g_1(\boldsymbol{X}) &= b_g - b_{g\,min}\ , \quad g_2(\boldsymbol{X}) = b_{g\,max} - b_g \\ g_3(\boldsymbol{X}) &= h_g - h_{g\,min}\ , \quad g_4(\boldsymbol{X}) = h_{g\,max} - h_g \\ g_5(\boldsymbol{X}) &= n_g - n_{g\,min}\ , \quad g_6(\boldsymbol{X}) = n_{g\,max} - n_g \\ g_7(\boldsymbol{X}) &= \frac{T}{R(1 - n_g b_g / W)} - p_{cr} \end{aligned}\right\} \quad \{28\}$$

In equations {27} and {28}, T_{slip} means the slip onset tension obtained from equation {17} and the last constraint function is imposed to protect the scratches due to high pressure at the top surface of grooves and groove corners, in which p_{cr} means the critical pressure to generate the scratches.

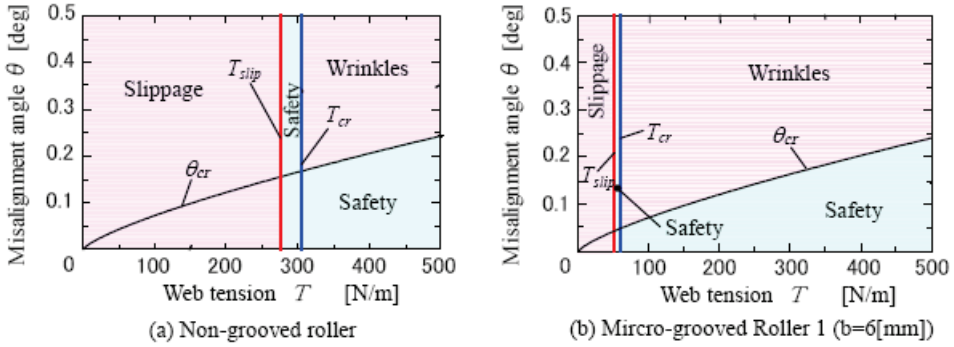

Figure **7** – Relation between slippage, wrinkling and safety regions
(U_r=0.3[m/s], W=0.3[m], Θ=60[deg], R=0.04[m], a=0.8[m])

EXPERIMENTS

To verify the applicability of prediction models proposed in this paper, the experiments on the generation of slippage and wrinkling were carried out for five types of rollers, one of which is the non-grooved roller, and the others are micro-grooved rollers. These micro-grooved rollers were designed and manufactured based on the micro-grooved roller theory developed in the former chapters including the optimum design. The upper and lower limits of b_g, h_g, n_g and the critical value of p_{cr} in equation {28} were predetermined as b_{gmin}=100μm, b_{gmax}=500μm, h_{gmin}=50μm, h_{gmax}=300μm, n_{gmin}=30, n_{gmax}=400 and p_{cr}=1.5kPa, respectively. The dimensions of designed micro-grooves are listed in Table 1, in which the cross section of groove was selected as triangle.

Item	Non-grooved	Groove1	Groove 2	Groove 3	Optimized
Groove pitch b, mm	—	6.0	3.0	2.1	1.0
Groove width b_g, μm	—	200	200	300	460
Groove depth h_g, μm	—	100	100	100	200
Groove number n_g	—	51	101	143	301
Roller roughness σ_r, μm	0.3	0.3	0.3	0.3	0.3

Table 1 – Dimension of test rollers

In the experiment on slippage, the experimental apparatus as shown in Figure 8 was used. One end of test web was glued to the other end over five rollers to form a loop that enables the endless transport of web. The web tension was set up step by step in the wide

range of tension from T=10N/m to T=210N/m. The roller surface velocity was continuously changed from U_r=0 to U_r=5m/s.

The web velocity and the roller surface velocity were, respectively, measured by the laser doppler velocimeter (LDV) at the same time, and after measuring these velocities the slip ratio defined by the following equation was calculated immediately.

$$s = \frac{|U_r - U_w|}{U_r} \qquad \{29\}$$

If the obtained slip ratio was larger than 0.01, we have judged the slippage was occurred between the web and roller, and the roller surface velocity at that time was defined and recorded as the slip onset velocity U_{slip}.

In the experiment on wrinkling, the same experimental apparatus as shown in Figure 8 was used, but the test roller was misaligned continuously from θ=0 to θ=1.5 deg in the horizontal plane, using a micro-screw until the wrinkling was completely generated in the web. The wrinkles generated on the roller surface were permanent deformation and did not recover, but the trough generated between the roller and roller was elastic deformation due to buckling and it could be recovered. Therefore, it was not difficult to distinguish the trough and wrinkling during the experiments.

When the wrinkling was occurred, the critical misalignment angle of roller, θ_{cr}, was immediately measured and recorded.

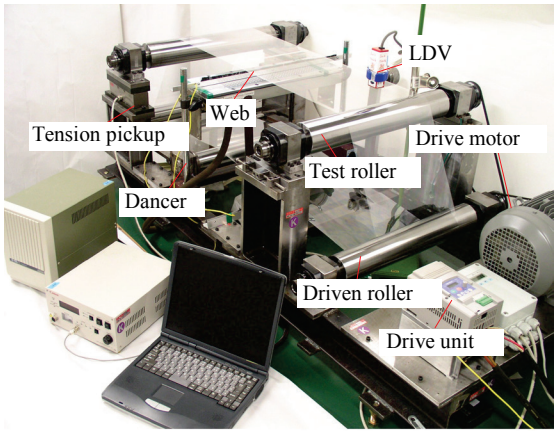

Figure 8 – Test apparatus for slippage and wrinkling

The physical properties of tested web are listed in Table 2.

Young's modulus in MD	E_x , Gpa	4.37
Young's modulus in CD	E_z , Gpa	4.29
Poisson's ratio in MD	ν_x	0.3
Poisson's ratio in CD	ν_z	0.3
Static friction coefficient	μ_s	0.3
Web thickness	t_w , μm	25
Web *rms* roughness	σ_w, μm	0.032

(MD: machine direction CD: cross machine direction)

Table 2 – Physical properties of tested web

RESULTS AND DISCUSSION

Figure 9 shows the relation between the slip onset velocity U_{slip} and web tension T for the fixed values of W=0.3m, Θ=60deg, R=0.04m, a=0.8m and θ=0(aligned roller) in which the plots show the measured data and the thick lines show the predicted results by equation {17}, respectively. The upper region of each line is corresponding to the slippage region and the lower region is corresponding to the non-slippage region, respectively. As can be seen in the figure, the slip onset velocity of micro-grooved roller with smaller groove pitch becomes higher than that of non-grooved roller. Especially, in the case of the optimized micro-grooved roller, no slippage and scratch could be seen during the experiments. The slip onset velocity increases drastically even in the case of very low tension. As a result, the micro-grooved roller, especially the optimized micro-grooved roller, is very much effective to prevent the slippage and scratches between the web and roller under the high transport speed with low web tension. In the figure, the predicted results agree well with the measured data, and then the applicability of the micro-grooved roller theory proposed in this paper is verified experimentally.

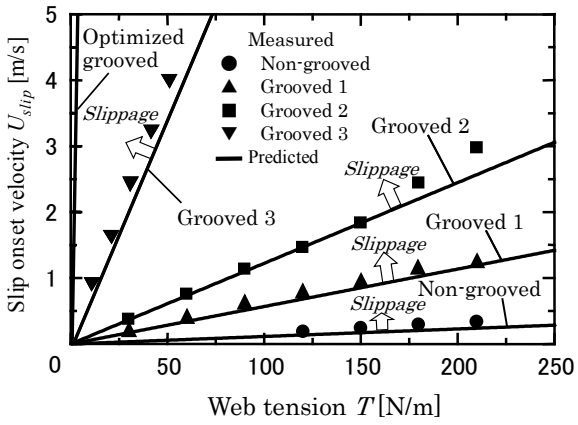

Figure 9 – Relation between slip onset velocity and web tension
(W=0.3[m], Θ=60[deg], R=0.04[m] , a=0.8[m], θ =0)

Figure 10 shows the theoretical prediction of the slippage region, wrinkling region and the safety operation region without both slippage and wrinkling accompanied with the measured data, in which the black plots mean the generation of wrinkling and the white plots mean the onset of slippage, respectively. It should be noticed that the horizontal axis

(web tension) in Figure 10(b) through 10(d) is half scale of that in Figure 10(a), and the calculated value of the critical misalignment angle θ_{cr} is the same for all cases. As can be seen in the figure, the slip onset tension T_{slip} of the micro-grooved roller decreases considerably and the slippage region becomes smaller with a decrease of groove pitch, especially the slip onset tension of the optimized micro-grooved roller approaches zero and there is no slippage region.

On the other hand, the critical tension to start the wrinkling T_{cr} of the micro-grooved roller also decreases and wrinkling region becomes larger with a decrease of groove pitch. As a result, the safety operation region becomes smaller as shown in Figures 10(b) and 10(c). This fact shows the strong trade-off relation between the slippage and wrinkling, so it is required to optimize the micro-groove sizes to enlarge the safety operation region as much as possible. Figure 10(d) shows the effectiveness of the optimized grooved roller that was designed by the optimization method proposed in this paper. In this case, the safety operation region becomes much larger than the other micro-grooved rollers shown in Figures 10(b) and (c). Especially at the conditions of high speed and low tension, which is the present and future trend in the handling of very thin, high functional webs, the effectiveness of the optimized micro-grooved roller is remarkable compared to the other rollers including non-grooved roller. There are reasonable agreements between the predicted results and the measured data.

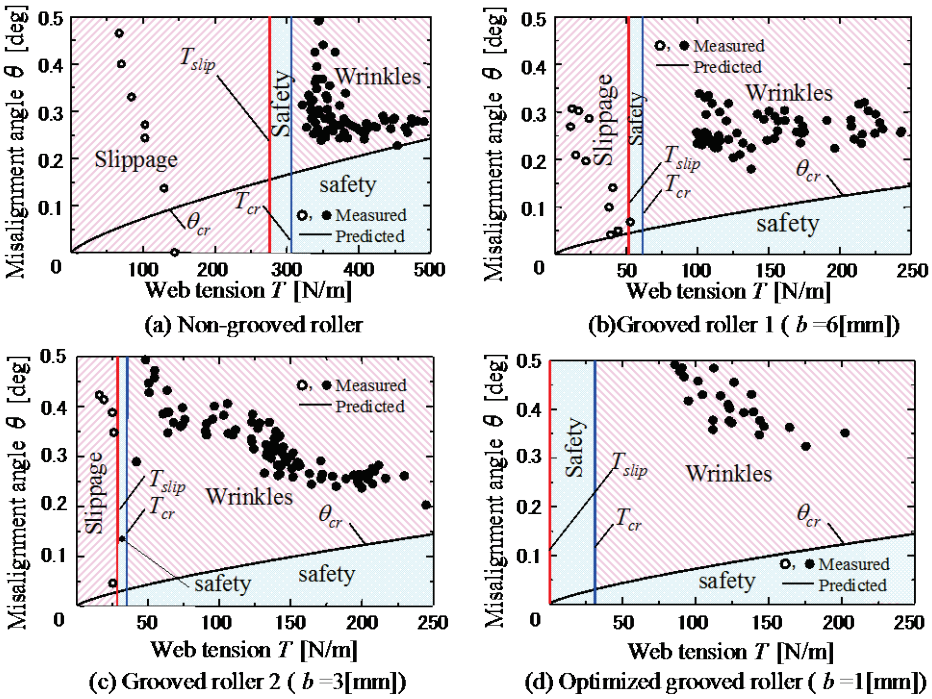

Figure 10 – Predicted and measured results of wrinkling and slippage
(U_r=0.3[m/s], W=0.3[m], Θ=60[deg], R=0.04[m], a=0.8[m])

APPLICATION TO PRODUCTION LIN

In the actual production lines of webs, many rollers are used for the transport of webs. Normally bearing torque is designed as much smaller than the traction torque, because the tension at the down stream of web line becomes much larger than that at the up stream, even if each bearing torque of rollers is less than 10^{-2}Nm. At this condition thin web will be expanded in the machine direction. In the present experiments carried out on the actual production lines, some break torque was added to the non-driven roller, and under the condition that the roller velocity was just 99.7% of the web velocity, namely slip ratio $s = 0.003$, break torque fr was measured as slippage torque. From the measured value of fr, and predetermined values of web tension T, and wrap angle Θ, the effective friction coefficient μ_{eff} was calculated by equation {16}. Figure 11 shows a comparison between the friction coefficient for the optimized micro-grooved roller and those for the non-optimized micro-grooved and non-grooved rollers. The optimized micro-grooved roller in the production line has almost the same groove sizes of the optimized micro-groove as shown in Table 1, although the triangle groove shape and surface roughness are different. The optimized micro-grooved roller exhibits a high friction coefficient, and it causes no slippage even at an increased roller velocity with very low tension of 40N/m. On the other hand, the friction coefficient for the non-optimized micro-grooved roller decreases as the web velocity increases. As can be seen in the figure, the optimized micro-grooved roller is very effective in the actual production line of webs.

On the other hand, in the actual production lines of webs, in order to increase the slip onset velocity, the non-driven rollers fabricated as light as possible are generally used to minimize resistance torque, which is equivalent to $I\dot{\omega} + fr$ as already introduced in equation {13}. However, when the weight of roller is reduced, the roller rigidity decreases at the same time and the roller will be bended by the tension, which leads to the generation of wrinkles similar to the wrinkles due to the misalignment of roller as already shown in Figure 6. To avoid such type of wrinkles, it has been well known experimentally to use the concave roller as shown in Figure 12, because the concave roller has a function to expand the web in the axial direction of roller. Therefore, combining the idea of micro-groove and concave roller, which means the use of the concave roller with micro-grooves, we can expect to prevent both slippage and wrinkling simultaneously even in the case of very high speed and low tension transport of webs.

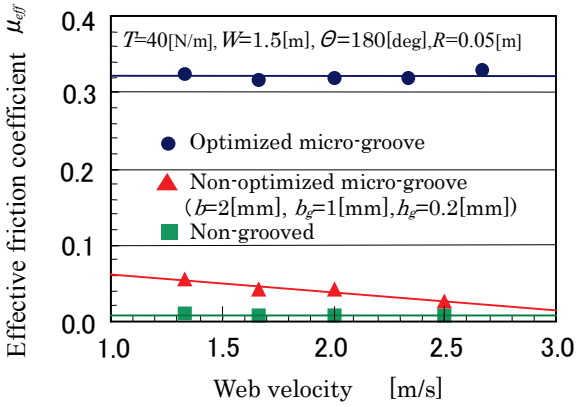

Figure 11 – Effective friction coefficients for three types of rollers in production line

Figure 12 shows the evidence of the effectiveness of the concave roller with optimized micro-grooves in the actual production line of webs. As can be seen in the figure, the wrinkling onset tension for the concave roller with the optimized micro-grooves became double compared to that for the straight roller with the same size of grooves. At that time, no slippage could be seen between the web and roller. From this fact, it was confirmed that combining the concave roller and the optimized micro-groove is very effective to transport the web without slippage and wrinkling under high velocity and low tension.

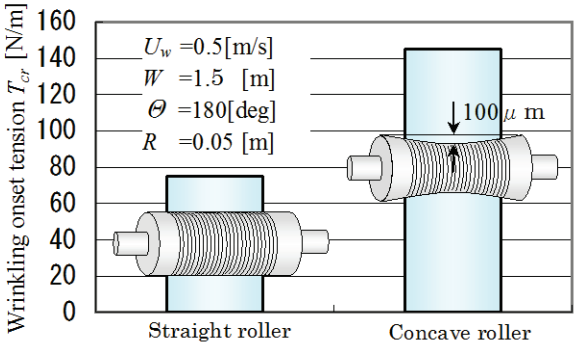

Figure 12 – Comparison of wrinkling onset tensions in production line

CONCLUSION

In this study, a theoretical model for predicting slippage and wrinkling between the web and micro-grooved roller was newly formulated, and the effectiveness of the model was verified experimentally. The main conclusions are summarized as follows.
The results based on the theoretical model for predicting the onset of slippage between the web and micro-grooved roller agree well with the experimental results.
The results based on the theoretical model for predicting the onset of wrinkling reasonably agree with the experimental results.
It was verified theoretically and experimentally that the optimized micro-grooved roller enables to enlarge the safety transport region without slippage and wrinkling.

Combining the concave roller and the optimized micro-groove, the safety transport region of webs is remarkably enlarged compared to the case of conclusion (3).

REFERENCES

1. Hashimoto, H. and Nakagawa, H., "Improvement of Web Spacing and Friction Characteristics by Two Types of Stationary Guides," Trans. ASME, Journal of Tribology, Vol. 123, 2001, pp.509-516.
2. Good, J. K., Kedl, D. M., and Shelton, J. J., "Shear Wrinkling in Isolated Spans," Proceedings of 4th International Conference on Web Handling, 1997, pp.462-479.
3. Hashimoto, H., "Prediction Model of Paper-web Wrinkling and Some Numerical Calculation Examples with Experimental Verifications," Journal of Microsystem Technology, 13, 2007, pp.933-941.

Improvement of Slippage and Wrinkling of Transporting Webs Using Micro-Grooved Rollers	**H. Hashimoto[1] and S. Hikita[2],** [1]Tokai University, [2]Fujifilm Corporation, JAPAN

Name & Affiliation	**Question**
Steve Lange, Procter & Gamble	Did you measure at all the lateral position of the web during your experiments for the different rolls?
Name & Affiliation	**Answer**
Hiromu Hashimoto, Tokai University	In our video examples you saw lateral motion. The lateral motion is not caused by slippage in the lateral direction. In our tests the web is in the form of a belt or loop and the splice generates transient lateral motion. If we use a straight web the splice error will be removed. Then there is no slippage because the friction force remains sufficient because there is no air entrainment due to the microgrooves.
Name & Affiliation	**Question**
Steve Lance, Procter & Gamble	So you didn't see a difference between the concave roller and the cylindrical rollers in terms of lateral position?
Name & Affiliation	**Answer**
Hiromu Hashimoto, Tokai University	We tried to observe the lateral motion for three types of rollers. The concave roller produces a spreading effect and there was no lateral motion for that case. For the case of a crown roller with microgrooves lateral motion was observed toward the center line and it was easy to generate wrinkles. For the case of a cylindrical roller we witnessed wrinkling due to the roller misalignment under high tension.
Name & Affiliation	**Question**
Bob Lucas, Winder Science	I have a question relative to your positive and negative crown rolls for centering or for spreading. You are introducing web/roller velocity differences at different locations on these rollers. Is there any evidence of micro-slip that would damage the surface of the web product?
Name & Affiliation	**Answer**
Hiromu Hashimoto, Tokai University	We experienced some scratches due to the microgrooves. We had to modify the microgrooves to protect the web from slippage and scratching. The groove edges must be rounded to prevent scratching.
Name & Affiliation	**Question**
Ron Swanson, 3M Company	Your paper does not list the third roller, the optimized roller.
Name & Affiliation	**Answer**
Hiromu Hashimoto, Tokai University	I am very sorry. If possible, I will add the details of the optimized roller after this conference.